Supporting Information

Two-dimensional honeycomb Coordination Network Based on Fused Triacontanuclear Heterometallic $\{Co_{12}Mn_{18}\}$ Wheels

Jiang Liu,[a] Mei Qu,[a] Rodolphe Clérac[b,c] and Xian Ming Zhang[a]**

[a]*School of chemistry & Material Science, Shanxi Normal University, Linfen, 041004, P. R. China. E-mail: zhangxm@dns.sxnu.edu.cn*

[b] *CNRS, CRPP, UPR 8641, F-33600 Pessac, France. E-mail: clerac@crpp-bordeaux.cnrs.fr*

[c]*Univ. Bordeaux, CRPP, UPR 8641, F-33600 Pessac, France*

Experimental Section

Crystal structure determination: The diffraction data of **1** were collected at 293 K on a Bruker Apex diffractometer (Mo-Kα, λ = 0.71073 Å). Lorentz-polarization and absorption corrections were applied. The structures were solved with direct methods and refined with the full matrix least-squares technique (SHELX-97). Analytical expressions of neutral-atom scattering factors were employed, and anomalous dispersion corrections were incorporated. All non-hydrogen atoms were refined anisotropically. Hydrogen atoms of organic ligands were geometrically placed and refined with isotropic temperature factors (Table S1).

Physical measurements: Elemental analyses were performed on a Perkin-Elmer 240 elemental analyzer. The FT-IR spectra were recorded on KBr pellets in the 400 to 4000 cm^{-1} range on a Nicolet 5DX spectrometer. The magnetic susceptibility measurements were obtained with the use of MPMS-XL Quantum Design SQUID magnetometer. This magnetometer works between 1.85 and 400 K for *dc* applied fields ranging from -7 to 7 T. Measurements were performed on a polycrystalline sample of 11.25 mg introduced in a polyethylene bag (3 × 0.5 × 0.02 cm). *M* vs *H* measurements have been performed at 100 K to check for the presence of ferromagnetic impurities that has been found absent. The magnetic data were corrected for the sample holder and the diamagnetic contribution.

Table S1. Crystallographic parameters for **1**

Compound	**1**
Empirical formula	$C_{36}H_{24}Co_3Mn_3N_{17}NaO_{19}$
Formula weight	1363.3
Crystal system	Trigonal
Space group	*R*-3
a (Å)	17.3430(7)
b (Å)	17.3430(7)
c (Å)	31.6652(19)
α (°)	90
β (°)	90
γ (°)	120
V (Å^3)	8248.2(7)
Z	6
$\rho_{calc,}$(g cm^{-3})	1.714
μ (mm^{-1})	1.651
F(000)	4082.5777
Crystal size (mm)	0.26 × 0.18 × 0.18
Reflections	6778 / 3230
R_{int}	0.0329
T_{max} /T_{min}	0.8635 / 0.6542
Data/parameters	3230 / 18 / 271
S	1.064
R_1[a], wR_2[b][$I > 2\sigma(I)$]	0.0883 / 0.2323
R_1, wR_2 (all data)	0.1240 / 0.2618
$\Delta\rho_{max}$/ $\Delta\rho_{min}$ (eÅ^{-3})	1.24 / -1.71

[a]$R_1 = \sum| |F_o| - |F_c| | / \sum |F_o|$. [b]$wR_2 = [\sum[w(F_o^2-F_c^2)^2]/\sum[w(F_o^2)^2]]^{1/2}$

Table S2. Selected bond lengths [Å] and angles [°] for **1**

Co1-O2	2.098(5)	Na3-O3	2.183(9)
Co1-O4	2.058(6)	Na3-O(3e)	2.183(8)
Co1-N1	2.107(8)	Na3-O(3f)	2.183(8)
Co1-N2	2.110(8)	Na3-N7	2.772(13)
Co1-N(3a)	2.173(7)	Na3-O(7e)	2.341(13)
Co1-N3	2.113(7)	Na3-O(7f)	2.341(13)
Mn2-O1	2.143(7)	Na3-O7	2.341(13)
Mn2-O(2b)	2.176(6)	N3-Co(1a)	2.173(7)
Mn2-O(4c)	2.251(8)	N3-Mn(2g)	2.484(7)
Mn2-O5	2.193(4)	O4-Mn(2h)	2.251(8)
Mn2-O8	2.244(8)	O5-Mn(2g)	2.193(4)
Mn2-N(3b)	2.484(7)	O5-Mn(2b)	2.193(4)
O2-Co1-N1	77.4(3)	O3-Na3-O7	108.9(6)
O2-Co1-N2	104.1(3)	O(3f)-Na3-O7	102.6(6)
O2-Co1-N3	83.3(3)	O3-Na3-O(7f)	145.8(5)
O2-Co1-N(3a)	94.3(2)	O(3e)-Na3-O(7f)	102.6(6)
O4-Co1-O2	177.4(3)	O(7e)-Na3-N7	25.8(3)
O4-Co1-N1	103.3(3)	O(7f)-Na3-N7	25.8(3)
O4-Co1-N2	78.4(3)	O7-Na3-N7	25.8(3)
O4-Co1-N3	95.8(3)	O7-Na3-O(7f)	44.4(5)
O4-Co1-N(3a)	83.1(3)	O7-Na3-O(7e)	44.4(5)
N1-Co1-N2	91.2(3)	C6-O1-Mn2	131.0(6)
N1-Co1-N(3a)	93.8(3)	Co1-O2-Mn(2g)	106.8(3)
N1-Co1-N3	160.6(3)	C6-O2-Co1	116.9(5)
N2-Co1-N(3a)	161.5(3)	C6-O2-Mn(2g)	136.2(5)
N2-Co1-N3	95.9(3)	C13-O3-Na3	155.3(9)
N3-Co1-N(3a)	85.0(3)	Co1-O4-Mn(2h)	107.7(3)
O1-Mn2-O(2b)	153.5(2)	C13-O4-Co1	118.7(7)
O1-Mn2-O(4c)	94.0(3)	C13-O4-Mn(2h)	133.1(7)
O1-Mn2-O5	102.89(18)	Mn2-O5-Mn(2g)	109.7(3)
O1-Mn2-O8	84.4(3)	Mn(2b)-O5-Mn(2g)	109.7(3)
O1-Mn2-N(3b)	81.9(2)	Mn(2b)-O5-Mn2	109.7(3)
O(2b)-Mn2-O(4c)	88.0(2)	N6-O8-Mn2	124.9(8)
O(2b)-Mn2-O5	102.48(16)	C1-N1-Co1	127.9(7)
O(2b)-Mn2-O8	88.6(3)	C5-N1-Co1	114.3(6)
O(2b)-Mn2-N3(b)	73.5(2)	C8-N2-Co1	126.5(8)
O(4c)-Mn2-N(3b)	72.6(2)	C12-N2-Co1	110.4(8)
O5-Mn2-O(4c)	102.2(3)	Co1-N3-Co(1a)	95.0(3)
O5-Mn2-O8	88.8(3)	Co1-N3-Mn(2g)	96.2(3)
O5-Mn2-N(3b)	173.3(3)	Co(1a)-N3-Mn(2g)	96.6(3)
O8-Mn2-O(4c)	168.9(3)	N4-N3-Co1	122.7(6)

O8-Mn2-N(3b)	96.3(3)	N4-N3-Co(1a)	116.2(6)
O(3f)-Na3-O3	96.6(4)	N4-N3-Mn(2g)	123.8(5)
O(3f)-Na3-N7	120.5(3)	O6-N7-Na3	180.000(3)
O3-Na3-N7	120.5(3)	O7-N7-Na3	56.9(7)
O(3f)-Na3-O(7e)	145.8(5)	O(7f)-N7-Na3	56.9(7)
O(3e)-Na3-O(7e)	108.9(6)	O(7e)-N7-Na3	56.9(7)
O3-Na3-O(7e)	102.6(6)	N7-O7-Na3	97.3(9)
O(3e)-Na3-O7	145.8(5)	O(7e)-O7-Na3	67.8(3)

Symmetry codes: a)4/3-x,5/3-y,2/3-z;b)2-y,1+x-y,+z; c)1/3+y,2/3-x+y,2/3-z; d)1-x,1-y,1-z; e)+y-x,1-x,+z; f)1-y,1+x-y,+z; g)1+y-x,2-x,+z; h)1/3-y+x,-1/3+x,2/3-z.

Table S3. BVS calculations for the Mn and Co ions in complex 1

Atom	Mn^{II}	Mn^{III}	Mn^{IV}	Oxidation
Mn	1.85	1.72	1.69	Mn^{II}
Atom	Co^{II}	Co^{III}	Co^{IV}	Oxidation
Co	2.36	2.21	----	Co^{II}

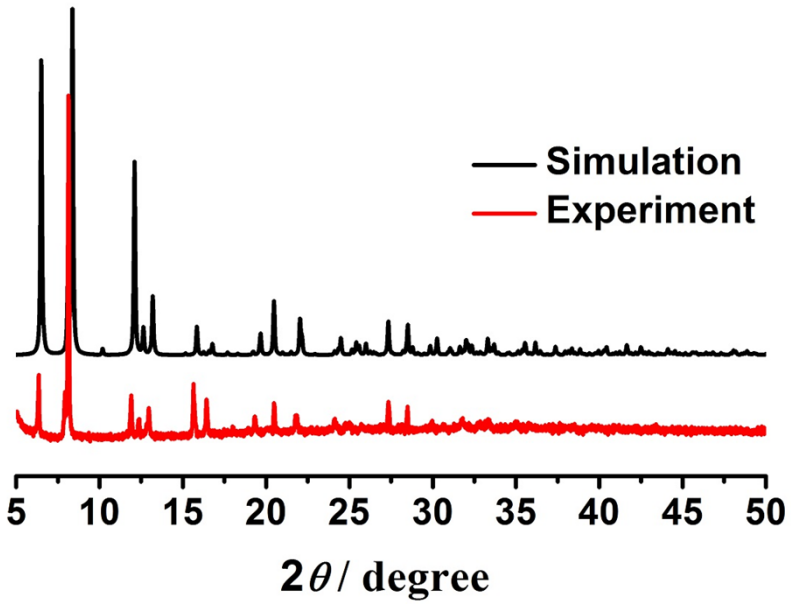

Figure S1. Experimental (red) and simulated (black) powder X-ray diffraction patterns for complex **1.**

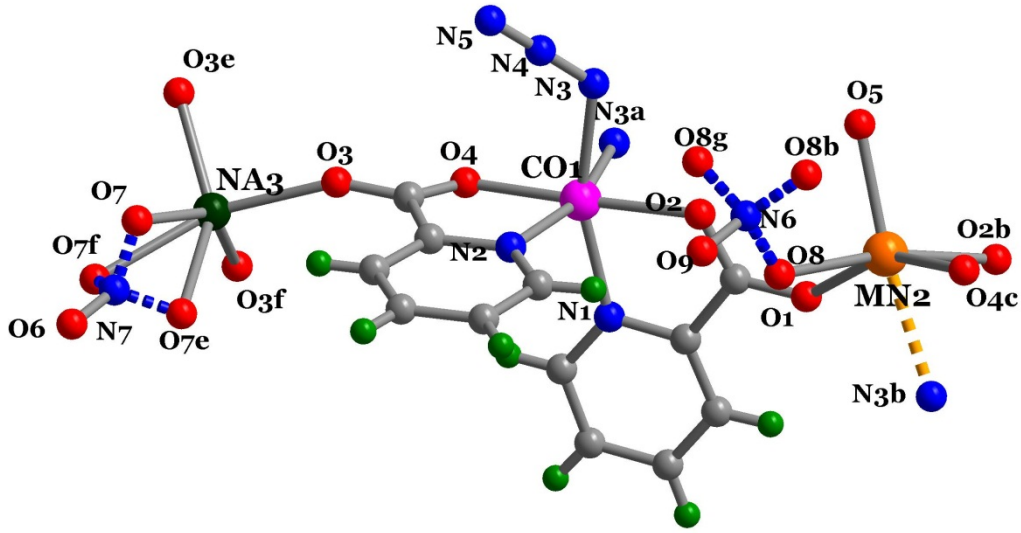

Figure S2. Coordination environments of the metal ions in **1**. The bonds involving disordered oxygen atoms from nitrates are shown in dashed blue lines. The weak Mn-N bond of 2.485 Å is shown in dashed yellow line.

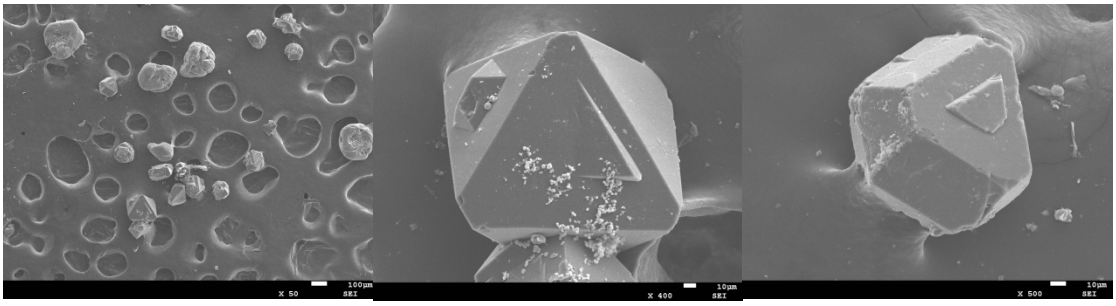

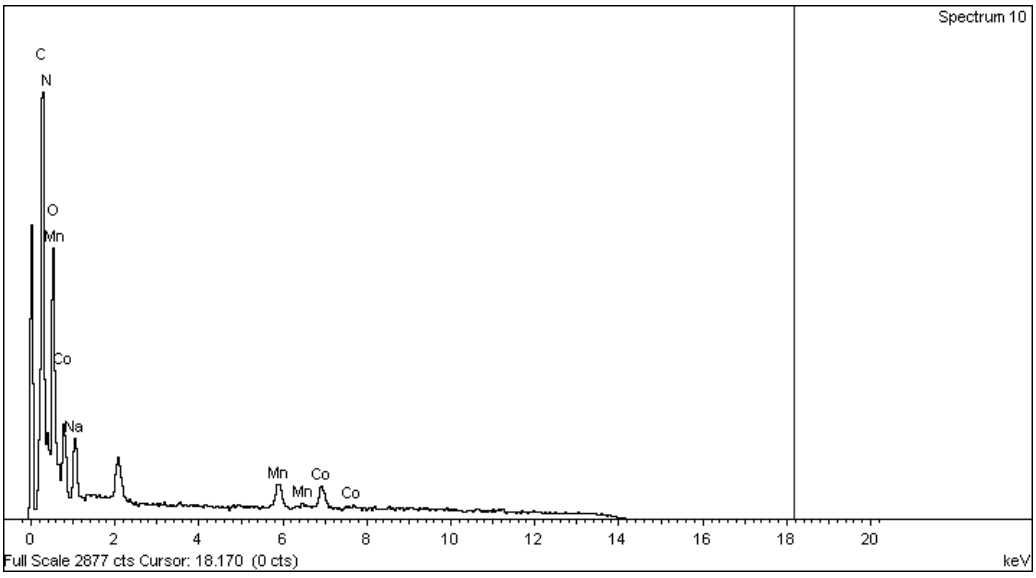

Figure S3. The EDS characterization for **1**.

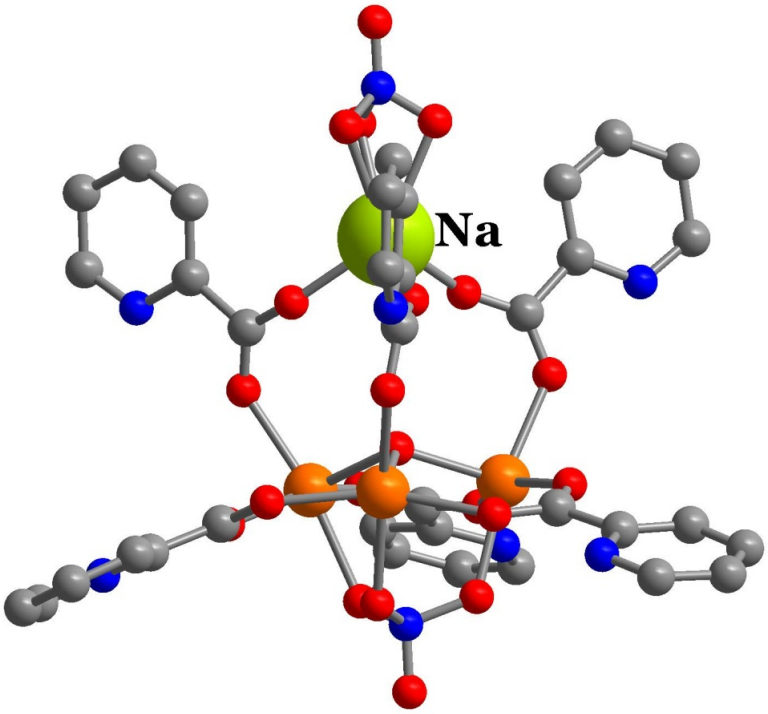

Figure S4. The view of $[Mn_3O(pic)_6(NO_3)]^{3-}$ unit showing calixarene-like hydrophilic cavity accommodated by Na^+ and additional nitrate.

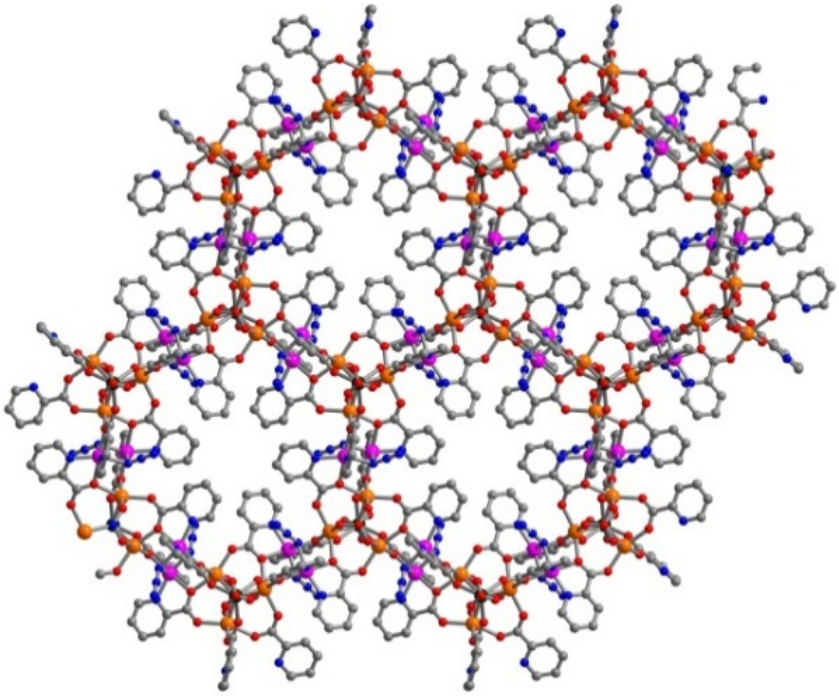

Figure S5. View of the 2-D coordination network $[Co_3(Mn_3O)(pic)_6(N_3)_3(NO_3)]^-$. Color code: Co purple, Mn orange, Na dark green, O red, N blue, C grey. Hydrogen atoms have been omitted for clarity.

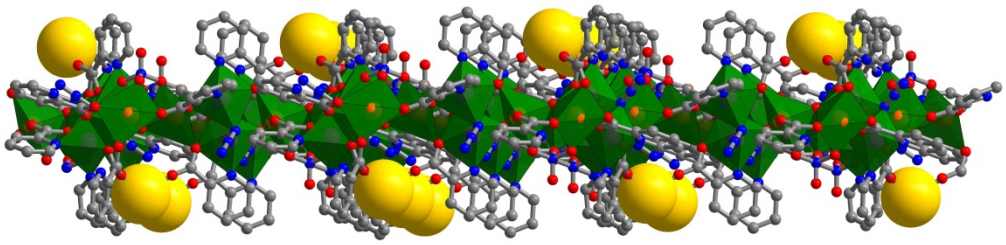

Figure S6. View of the interlayer multiple calixarene-like hydrophilic cavities yellow balls) created by picolinate ligands in combination with $[Mn_3O]^{4-}$ units.

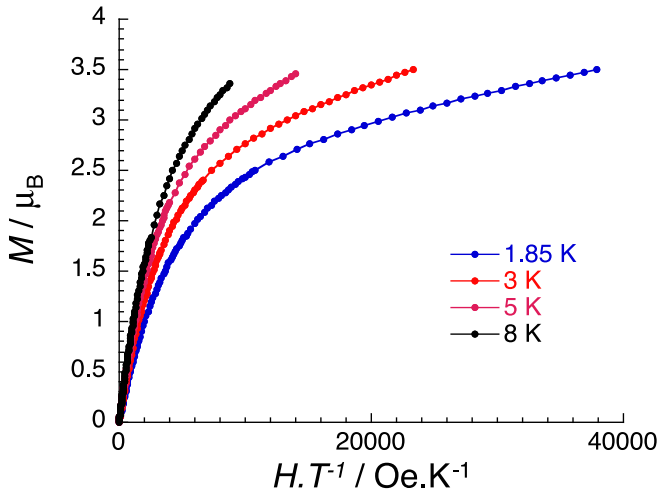

Figure S7. *M* vs *H/T* plot for **1** with applied dc field up to 7 T.

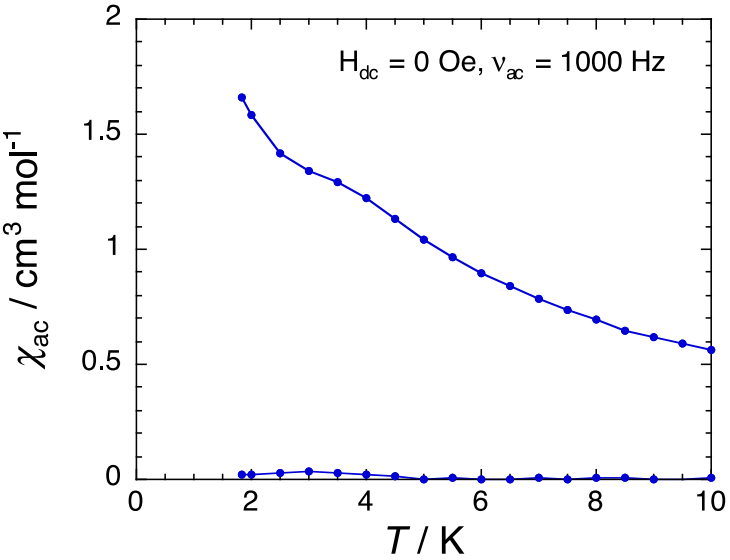

Figure S8. Temperature dependence below 10 K of the real (χ' top) and imaginary (χ", bottom) parts of the ac susceptibility for **1** in zero dc-field at 1000 Hz. Solid lines are guides.